CHAPTER 4

Migration of Common Midpoint Snell Traces

4.1. Introduction

A *Snell trace* is a radial trace generalized to depth variable velocity. It is extracted from an approximately diagonal path across a CMP gather (Figure 4.1), but may curve depending on the velocity function. The trajectory is characterized by a given ray parameter, hence it's name. We migrate sections composed of a Snell trace taken from each common midpoint (CMP) gather.

The method of Snell trace migration borrows from both radial traces and slant stacks. Like radial traces, it extracts angle-midpoint sections from the seismic data directly. Thus it acquires most of the practical advantages of radial traces. Like slant stacks, Snell traces map a CMP gather into portions with the same ray parameter, i.e. moveout slope. This gives Snell traces the power to handle depth variable velocity.

4.2. Mathematical Description of A Snell Trace

A Snell trace is defined as the line formed by the places on a CMP gather where hyperbolic reflections from flat reflectors have the same slope. From the mathematical description of slant stacking (section 2.3), this slope is proportional to the ray parameter p. The hyperbolic reflections are computed for flat reflectors and take into account depth variable velocity.

The traveltime to a flat reflector in a CMP gather is

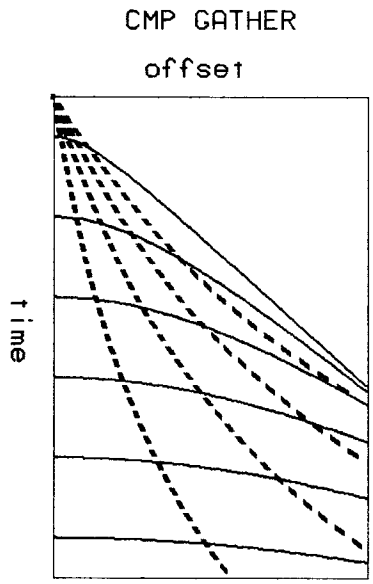

FIGURE 4.1: Common Midpoint Snell traces. A Snell trace (dashed line) is extracted from a CMP gather where the reflection hyperbolas (thick lines) all have the same slope. Snell traces for several different ray parameters are shown, with the ray parameter increasing towards the right. A Snell trace is straight if the velocity is constant. Here they bend upward because the velocity increases with depth.

$$t = \left(t_0^2 + \frac{4h^2}{v^2} \right)^{1/2} \tag{4.1}$$

assuming a constant velocity and where t_0 is the reflection time at zero offset. The reflection slope on CMP gather is $\partial h / \partial t$. Setting this proportional to the ray parameter gives

$$\frac{\partial t}{\partial h} = 2p = \frac{4h}{v^2 t} \tag{4.2}$$

We solve equations (4.1) and (4.2) to find the time and offset positions of these reflector slopes, and hence the Snell trace trajectory.

$$h = \frac{pv^2 t_0}{2} \left(1 - p^2 v^2 \right)^{1/2} \tag{4.3}$$

$$t = t_0 \left(1 - p^2 v^2 \right)^{-1/2} \tag{4.4}$$

We have written offset and time in terms of t_0 and p in order to make it easy to

generalize to depth variable velocity. Zero offset time t_0 is directly proportional to depth by $dz = v dt_0/2$. ray parameter p is an invariant with depth according to Snell's law. We integrate equations (4.3) and (4.4) over thin constant velocity horizontal strata to obtain

$$h(z) = \int_0^z dz\, pv \left(1 - p^2 v^2\right)^{-1/2} \tag{4.5}$$

$$t(z) = 2 \int_0^z \frac{dz}{v} \left(1 - p^2 v^2\right)^{-1/2} \tag{4.6}$$

Equations (4.5) and (4.6) are used to map Snell traces from CMP gathers.

4.3. Migration Equation for Midpoint Snell Traces

The equation for migrating Snell traces proceeds directly from the equation for migrating radial traces (3.5).

$$\frac{\partial P}{\partial z} = -2i\frac{\omega}{v}\left(\frac{1 - Y^2}{1 - \frac{4r^2}{v^2}}\right)^{1/2} P \tag{3.5}$$

We convert the radial parameter r into ray parameter p by recalling the definition of r.

$$r = \frac{h}{t} \tag{3.2}$$

We substitute equation (4.2) into (3.2) to obtain the relation

$$r = \frac{pv^2}{2} \tag{4.7}$$

Substituting this equation into equation (3.5) gives an equation for migrating Snell traces

$$\frac{\partial P}{\partial z} = -2i\frac{\omega}{v}\left(\frac{1 - Y^2}{1 - p^2 v^2}\right)^{1/2} P \tag{4.8}$$

4.4. Velocity Analysis

Velocity analysis using Snell traces follows the same principles for pre-critical angle reflections on slant stacks. Only the equations are different.

Velocity analysis uses a gather of Snell traces made at the same midpoint, but for different ray parameters. These are called *Snell trace gathers*, an example of which is shown in Figure 4.2. Velocity analysis *before* migration uses an equation that gives time shifts as a function of velocity and ray parameter. Migration should convert all reflection times to zero offset (Figure 4.3). If not, the residual time shifts can be used to improve the velocity estimate.

4.5. Velocity Estimation Equations

A formula giving velocity as a function of time and and ray parameter on a Snell trace gather has already been derived as equation (4.6). Equation (4.6) correctly predicts that reflection times increase with ray parameter on a Snell trace gather (Figure 4.2).

The derivation of an equation for estimating velocity after migration from residual time shifts proceeds along the same steps as for slant stacks (section 2.7). First, we verify that the migration operator (4.8) converts Snell trace times to zero offset. Assuming that migration nullifies dip, then the dip dependent term Y in equation (4.8) can be ignored. Equation (4.8) is inverse Fourier transformed over time to give a time shifting equation that is the inverse of the Snell trace moveout (4.6).

$$\frac{\partial P}{\partial z} = \left[- \frac{2}{\hat{v}} \left(1 - p^2 \hat{v}^2 \right)^{-1/2} \right] \frac{\partial P}{\partial t} \tag{4.9}$$

$\hat{v}$ is the velocity used for migration. A formula for computing the actual velocity v is derived by comparing the migration time shift to the original time shift. The derivation parallels that of equations (2.17) to (2.21).

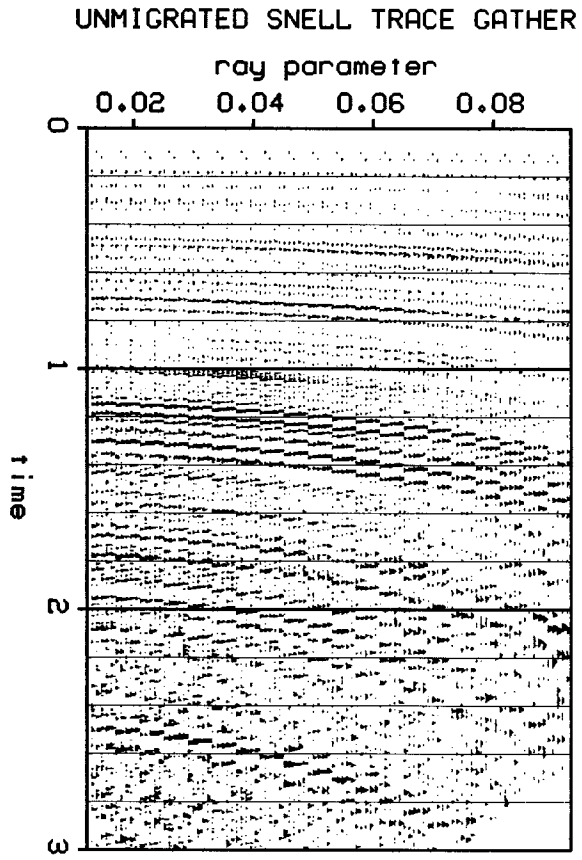

FIGURE 4.2: Unmigrated Snell trace gather. Collection of 20 Snell traces, each 5 midpoints wide, from midpoints 100 to 105 in Figure 4.4. This figure demonstrates how time increases with increasing ray parameter p. The smallest ray parameter is .015 and the interval is .004 millisecond/feet.

$$v = \left[\frac{\hat{z}_1^2(1 - p_2^2\hat{v}^2) - \hat{z}_2^2(1 - p_1^2\hat{v}^2)}{p_2^2\hat{z}_2^2(1 - p_1^2\hat{v}^2) - p_1^2\hat{z}_1^2(1 - p_2^2\hat{v}^2)} \right]^{1/2} \tag{4.10}$$

Equation (4.10) may be interpreted qualitatively in terms of the following chart

given $p_2 < p_1$:

undermigrated	$\hat{v} < v$	$\hat{z}_1 > \hat{z}_2$	increasing moveout
exact	$\hat{v} = v$	$z_1 = z_2$	no moveout
overmigrated	$\hat{v} > v$	$z_1 < z_2$	decreasing moveout

We have not found a closed form expression for estimating depth velocity variations.

Instead we use equation (4.10) to iteratively estimate thin constant velocity layers

in the earth.

4.6. Processing Sequence for Midpoint Snell Traces

A Snell trace migration sequence is:

(1) Construct Snell trace sections by assembling the Snell trace for a given p from each CMP gather. Appendix E gives advice on what range of ray parameters to use.

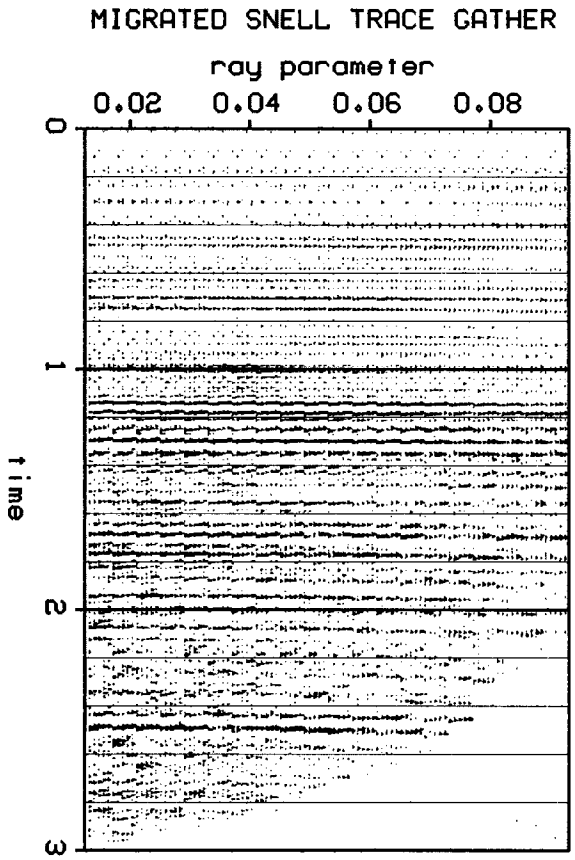

FIGURE 4.3: Migrated Snell trace gather. Same Snell trace gather as in Figure 4.2, except migrated. Because the migration velocity was nearly correct, the time of a reflector is about the same at any ray parameter.

(2) Second, migrate each Snell trace section using equation (4.8). A computer implementation of this equation is discussed in appendix G.

(3) Third, analyze migrated Snell trace gathers to improve velocity estimates.

(4) Finally, stack together one or more migrated sections. The main motivation is to improve signal to noise in the result. A second reason is that a portion of the dataset may be absent at one ray parameter, while present at another.

4.7. Results

Snell trace migration was used to image the growth fault dataset (Figure 4.4) and synthetic (Figures 4.5 - 4.7) appearing elsewhere in this thesis. Overall, it is quite successful in imaging steep dipping reflectors and regions where events of different dips coincide. Figure 4.7 shows that Snell traces succeed even where there are missing offsets.

4.8. Relationship of Snell Traces to Slant Stacks

A Snell trace is a hybrid between a radial trace and a slant stack. A Snell trace selects the same part of a CMP gather as a slant stack when there is no dip, given the same ray parameter. The reflection times on a slant stack and Snell trace are different. A equation to convert Snell traces into slant stacks is obtained by combining their individual moveout equations (2.15) and (4.6).

$$t = 2 \int_0^z \frac{dz}{v\left(1 - p^2 v^2\right)} \tag{4.11}$$

Snell traces and slant stack treat dipping events differently, though correctly. A slant stack captures a dipping event where it has the same slope as a flat event. This is at a wider offset than the Snell trace trajectory. The consequence is that equation (4.11) for converting Snell traces into slant stacks is inaccurate for dipping events. The different forms of the migration equations (Snell traces has a single

square root, slant stacks has a double square root) reflects the different way dipping events are treated.

Slant stacks are accurate beyond the critical angle, while Snell traces are not. A theory for lateral velocity variations has not been worked out for Snell traces.

It is easier to transform CMP gathers into Snell traces than into slant stacks. Truncation and aliasing are much less of a problem. The cost of making Snell traces is one interpolation per output point, whereas each slant stack output point is a sum (and possibly interpolation) of as many points as there are offsets. (The frequency domain slant stack method of appendix C reduces the cost of slant stacking somewhat.) Slant stacking may require costly pre-processing to reduce artifacts (Appendix B).

Because slant stacks are *stacks*, they reduce the noise level over raw data. Snell traces have the same noise level as raw data.

Unlike slant stacks and radial traces, Snell traces require some knowledge of a depth velocity model. However, Snell traces are not as sensitive to velocity error as is conventional stacking. A velocity error will degrade a reflector image on a CMP stack while just causing a timing error on a Snell trace.

4.9. Conclusions

Migrating midpoint Snell traces alleviates the steep dip and dip selectivity problem of migrating CMP stacks. Velocity estimation may be done after migration when the data quality has been improved. Snell trace migration is more accurate than radial trace migration and more practical than slant stack migration. The results are comparable to slant stack migration.

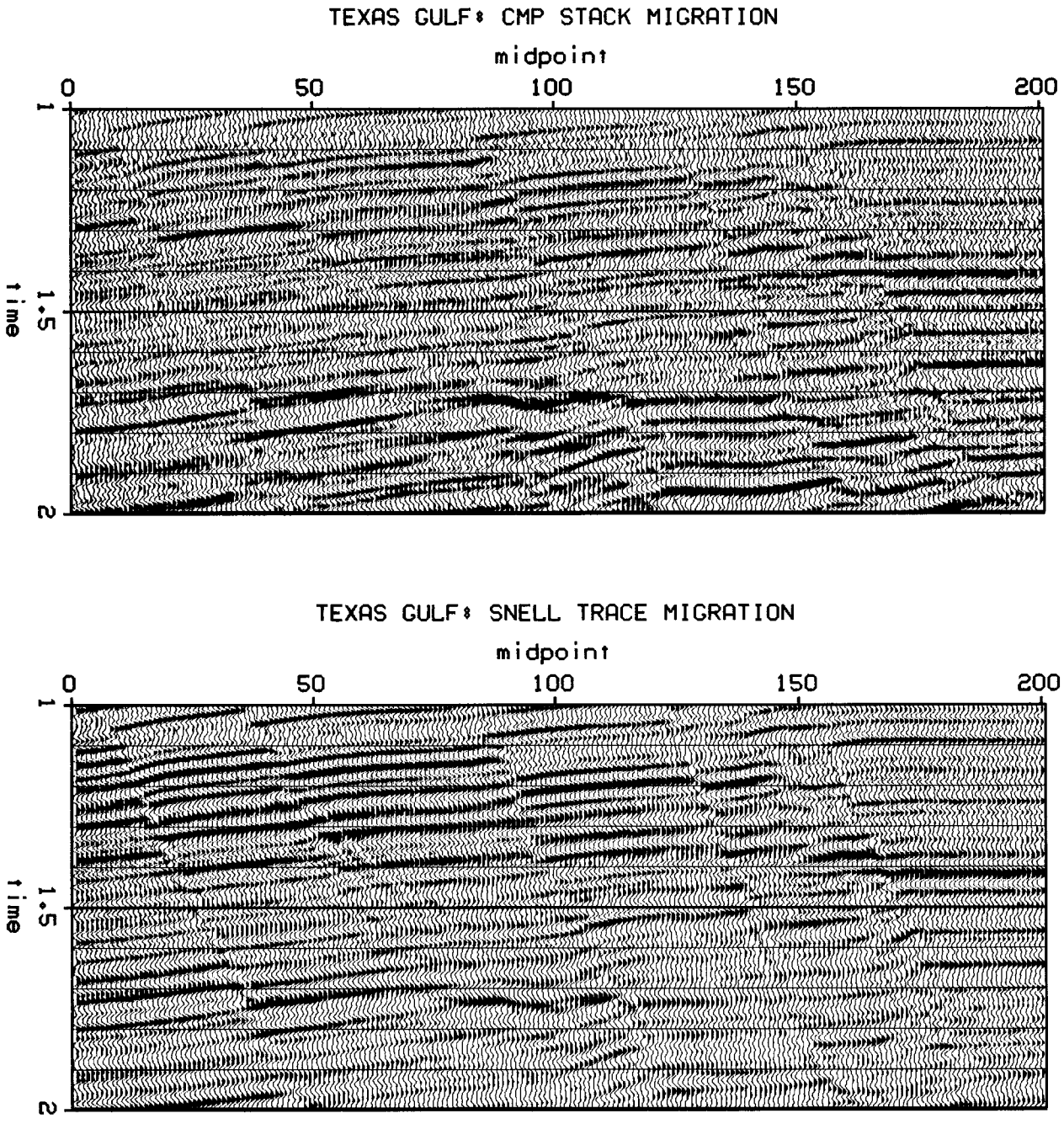

FIGURE 4.4: Snell trace migration vs. conventional migration. On the top is a CMP stack migration of a Gulf coast dataset. Below is the Snell trace migration of the same dataset. The fault plane reflections are imaged much better after Snell trace migration.

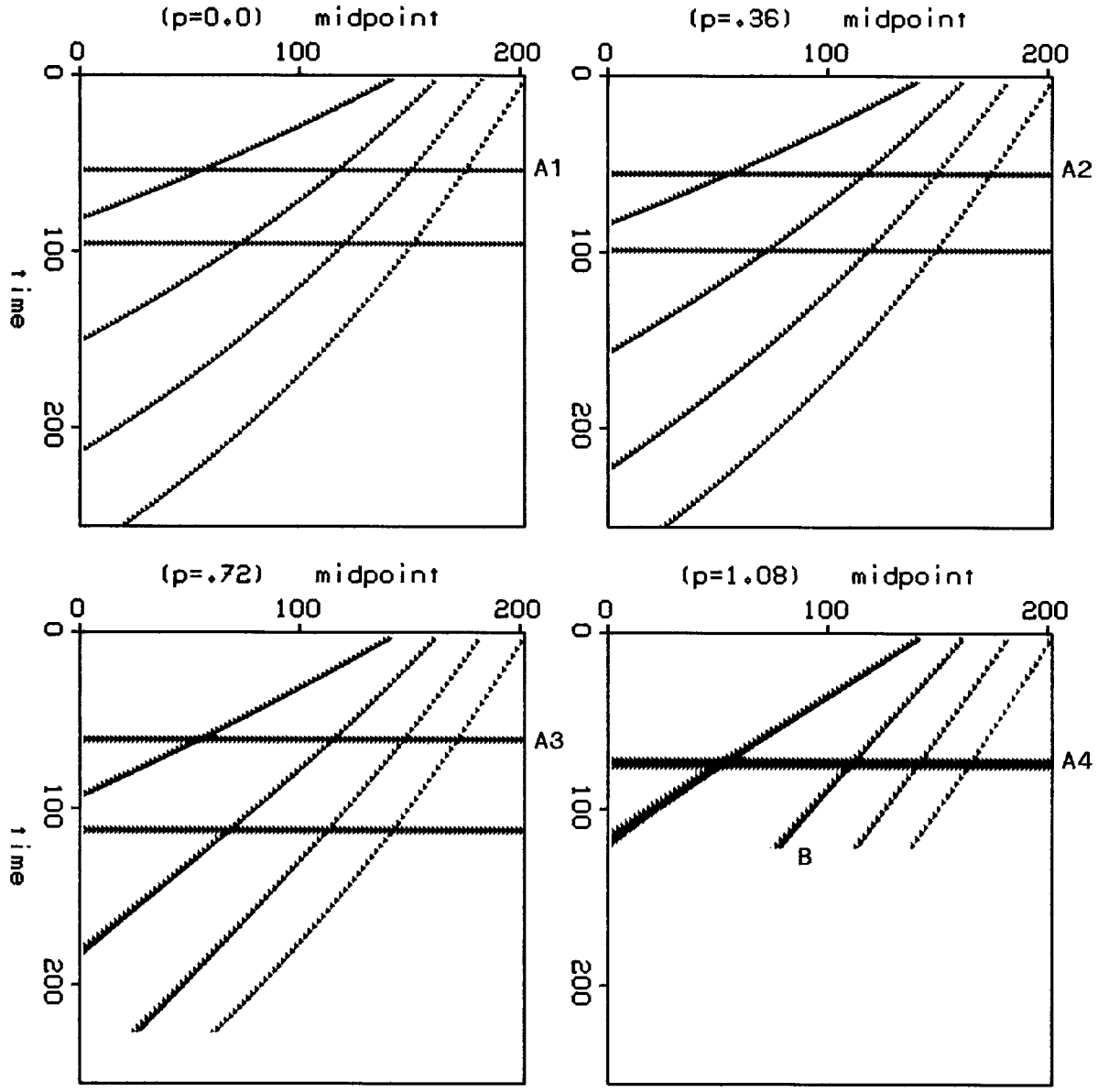

FIGURE 4.5: Synthetic Snell trace sections. These Snell traces sections are made from the linearly increasing depth velocity model of Figure 2.9. The ray parameter is given above each section. The purpose of this model is to test Snell trace migration at very steep dips (80°) and relatively wide offsets. Notice the increasing time moveout as the ray parameter increases (A1-A4). In the last panel, data is missing due to the wide offset cutoff (B).

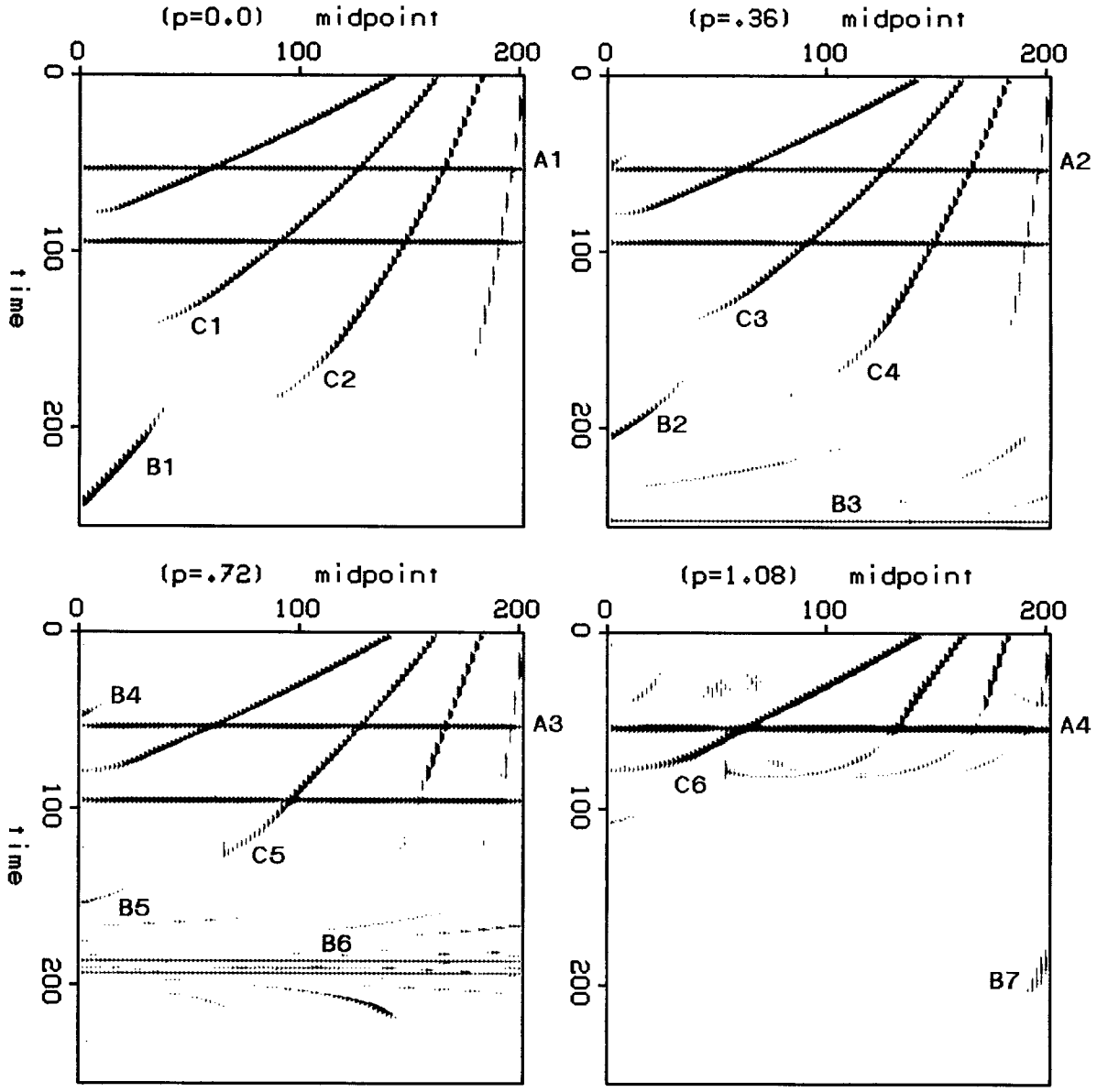

FIGURE 4.6: Migrated synthetic Snell trace sections. Time migrations of the Snell trace panels from the previous figure. These have not yet been converted to depth. Migration converts each panel into an earth image. Therefore, migration removes the travel time shifts from the unmigrated panels (A1-4). The curved lines are frequency domain wraparound (B1-7) and reflector truncation tails (C1-6). These are artifacts due to the specific computer implementation of the migration equation and not Snell trace migration itself.

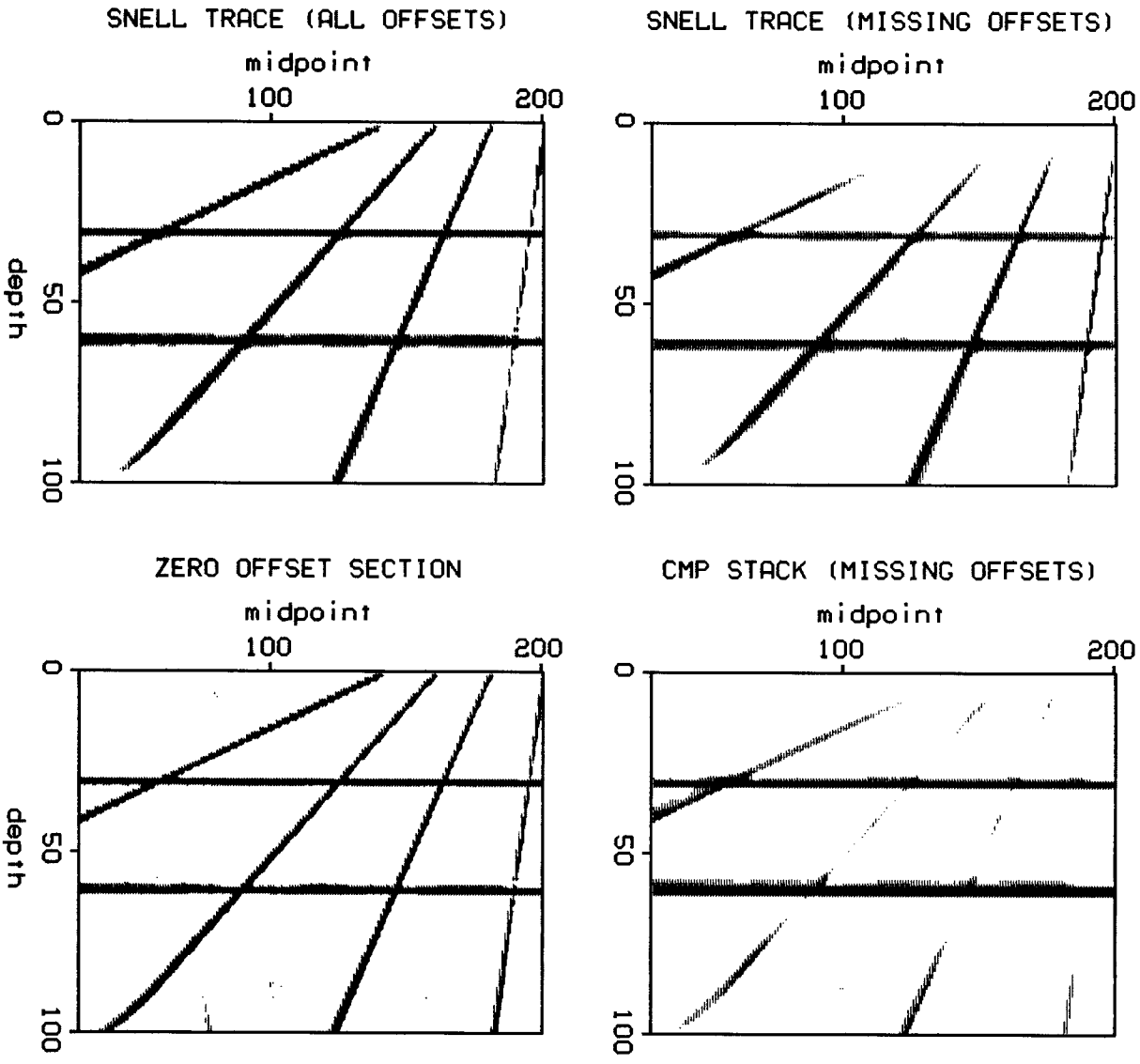

FIGURE 4.7: Migration comparisons. The upper left section is a sum of 50 migrated Snell trace sections. The upper right section is a sum of 45 migrated Snell trace sections where the ten inner CMP gather offsets were not included. Both results are comparable to the zero offset section migration in the lower left and much better than the CDP stack migration in the lower right. The tops of the right two migrations are missing due to missing inner offsets. The ray parameters ranged from 0. to 1.5 for the case with all the offsets and from .15 to 1.5 for the offset missing case. The interval between ray parameters increases by a geometric factor of 1.03 in both cases.